Biosensors and Bioelectronics 24 (2008) 22–28

Contents lists available at ScienceDirect

Biosensors and Bioelectronics

journal homepage: www.elsevier.com/locate/bios

Amperometric glucose biosensor based on layer-by-layer covalent attachment of AMWNTs and IO_4^--oxidized GOx

Yingying Sun, Haiying Wang, Changqing Sun*

College of Chemistry, Jilin University, Changchun 130012, PR China

ARTICLE INFO

Article history:
Received 28 January 2008
Received in revised form 9 March 2008
Accepted 11 March 2008
Available online 18 March 2008

Keywords:
Amino terminated carbon nanotubes
Layer-by-layer covalent attachment
Low-potential detection of the glucose
Glucose biosensors

ABSTRACT

Multi-wall carbon nanotubes (MWNTs) functionalized with amino groups were prepared via silane treatment using 3-aminopropyltrimethoxysilane (APS) as a silane-coupling agent. The resultant amino terminated MWNTs (AMWNTs) were applied to construct glucose biosensors with IO_4^--oxidized glucose oxidase (IO_4^--oxidized GOx) through the layer-by-layer (LBL) covalent self-assembly method without any cross-linker. Scanning electron microscopy (SEM) indicated that the assembled AMWNTs were almost in a form of small bundles or single nanotubes, and the surface density increased uniformly with the number of GOx/AMWNTs bilayers. From the analysis of voltammetric signals, a linear increment of the coverage of GOx per bilayer was estimated. The resulting biosensor showed excellent catalytic activity towards the electroreduction of dissolved oxygen at low overvoltage, based on which glucose concentration was monitored conveniently. The enzyme electrode exhibited good electrocatalytic response towards the glucose and that response increased with the number of GOx/AMWNTs bilayers, suggesting that the analytical performance such as sensitivity and detection limit of the glucose biosensors could be tuned to the desired level by adjusting the number of deposited GOx/AMWNTs bilayers. The biosensor constructed with four bilayers of GOx/AMWNTs showed high sensitivity of 7.46 μA mM^{-1} cm^{-2} and the detection limit of 8.0 μM, with a fast response less than 10 s. Because of relative low applied potential, the interference from other electro-oxidizable compounds was minimized, which improved the selectivity of the biosensors. Furthermore, the obtained enzyme electrodes also showed remarkable stability due to the covalent interaction between the GOx and AMWNTs.

1. Introduction

Since the first discovery in 1991 (Iijima, 1991), carbon nanotubes (CNTs) have attracted great research interest due to their high surface area, excellent electrical conductivity and unique chemical properties (Rao et al., 2001; Baughman et al., 2002). These remarkable properties make CNTs good candidates for nanoelectronic devices (Fuhrer et al., 2000), electron field emission sources (Fan et al., 1999), scanning probes (Wong et al., 1998) and especially biosensors (Wang et al., 2003b; Joshi et al., 2005; Huang et al., 2006). The structure of CNTs can be thought of conceptually as "rolled-up" sheets of graphite: a single rolled up graphene sheet forms single-wall carbon nanotubes (SWNTs), while several sheets of graphite rolled into concentric tubes form multi-wall carbon nanotubes (MWNTs). Recently, the combination of MWNTs and glucose oxidase (GOx) is receiving considerable interest. Many studies have proven that MWNTs are very suitable matrices to trap GOx for glucose biosensors with fast response time, high sensitivity, and great versatility (Wang and Musameh, 2003a; Joshi et al., 2005; Deng et al., 2007). Different approaches, such as physical direct adsorption of GOx on MWNTs (Guan et al., 2005), encapsulation (Salimi et al., 2004) and entrapment (Wang and Musameh, 2005) have been used to construct MWNTs/GOx biosensors. However, the drawback to these methods is non-uniform adsorption and GOx leaching from the films. Thus, the most important issues for preparing MWNTs/GOx biosensor should be mild conditions to functionalize MWNTs and a high efficiency to immobilize large quantities of GOx. Layer-by-layer (LBL) self-assembly based on electrostatic interaction has emerged as the most popular and versatile approach for the fabrication of organized multilayer films (Decher, 1997; Jiang and Tsukruk, 2006). It is a simple way to produce fundamentally and practically interesting multilayer films with unique mechanical properties and precise control over film composition and thickness, which opens many new opportunities for us to achieve the ideal model surface whose properties are controllable (Olek et al., 2004). Recently, this technique has found wide applications in preparation of MWNTs/GOx multilayer biosensors. For instance, Khor' group constructed MWNTs/GOx

* Corresponding author. Tel.: +86 43185167655; fax: +86 43185167655.
E-mail address: sunchq@mail.jlu.edu.cn (C. Sun).

0956-5663/$ – see front matter © 2008 Elsevier B.V. All rights reserved.
doi:10.1016/j.bios.2008.03.004

multilayer films through alternative electrostatic interaction of the positively charged PDDA with the oppositely charged MWNTs and GOx (Yan et al., 2007). Zhao and Ju (2006) also fabricated LBL films via the alternate deposition of PDDA-wrapped MWNTs and GOx on the Au electrodes. Despite successful fabrication has been realized, the driven force in those LBL assembly processes is electrostatic interaction, which certainly leads to the poor stability and the limited application. Besides, the polyelectrolytes employed to combine MWNTs with GOx increase the distance between the FAD center of GOx and nanotubes, which results in reduced electron-transfer rate and thus the poor analytical properties. To overcome these drawbacks, directly LBL covalent attachment of GOx on MWNTs without any cross-linker for fabricating multilayer films is a practical method.

In this paper, we report the chemical modification of MWNTs by covalent bonding of an amino terminated silane (3-aminopropyltrimethoxysilane, APS) onto activated carbon nanotubes. By using silane-coupling chemistry, the amino terminated MWNTs (AMWNTs) maintained the carbon skeleton structure, while grafting new functional groups. To our knowledge, only one study has been reported on the silane treatment of MWNTs with APS, but no function of the system was addressed (Shanmugharaj et al., 2007). Here we applied such AMWNTs to the construction of glucose biosensors. LBL method was employed for direct attachment of IO_4^--oxidized glucose oxidase (IO_4^--oxidized GOx) on the AMWNTs, based on the covalent Schiff-base bonding between the aldehyde groups of IO_4^--oxidized GOx and amino groups of AMWNTs. In this way, the polyelectrolytes and cross-linkers (e.g. glutaraldehyde) were avoided, and the thickness of multilayer films was in nanometer. The resulting electrode showed a porous structure and exhibited outstanding bioelectrocatalytic response to the oxidation of glucose. The AMWNTs involved can not only adsorb GOx without loss of biological activity but also facilitate the electron-transfer. Furthermore, the obtained biosensor had an excellent stability because of covalent interlayer bonding. The optimization and advantages of such GOx/AMWNTs biosensors are reported in the following sections.

2. Experimental

2.1. Reagents

Glucose oxidase (GOx, EC 1.1.3.4, from Aspergillus niger, 100 U mg^{-1}) was purchased from Amersco. 3-Aminopropyltrimethoxysilane (APS, 99%), cystamine dihydrochloride (CA) and ferrocenemethanol were obtained from Aldrich. Multi-wall carbon nanotubes (MWNTs, >95%, 10–30 nm diameter) came from Shenzhen Nanotech Port Ltd. Co. (Shenzhen, China). The other chemicals were of analytical grade and were used as supplied. All the solutions were prepared using doubly distilled water. 0.1 M phosphate buffer solutions (PBS, pH 6.82) were employed as supporting electrolyte.

To oxidize carbohydrate groups to the aldehydes on the peripheral surface of GOx, we followed a methodology already demonstrated by Zaborsky and Ogletree (1974), the details of which were described in our previous publications (Sun et al., 2007).

2.2. Instrumentation

Scanning electron microscope (SEM, SHIMADZU SSX-550) was used for imaging the morphology of the multilayer films.

A CHI 660B workstation was used to collect electrochemical data. Experiments were performed at room temperature ($25 \pm 1\,^{\circ}C$), in a conventional three-electrode system with 2.0-mm-diameter Au modified working electrode, a platinum wire as the auxiliary electrode, and a saturated calomel electrode (SCE) reference electrode. All of the potentials were reported versus this reference. The amperometric experiments were carried out in a gently stirred, air-saturated, 0.1 M PBS. The desired potential was applied, and the background current was allowed to decay to a constant level. The glucose stock solutions were prepared with 0.1 M PBS and were allowed to mutarotate overnight before use. Unless pointed out, the experiments were carried out in air-saturated solutions. An anaerobic condition was obtained by purging the solution with a high purity nitrogen gas for 20 min prior to the experiment and by maintaining a positive pressure of nitrogen during the experiment. All presented experimental results were the mean of at least three identically prepared electrodes, if not otherwise mentioned.

2.3. Silanization of MWNTs with APS

The process started by oxidizing as received MWNTs in 10 M H_2SO_4 containing 0.04 g mL^{-1} $K_2Cr_2O_7$ for 30 min at 80 °C. The aim of this treatment was to create oxygen-containing groups on nanotubes and also to remove the graphitic impurities that were present along with the MWNTs (Ravindran et al., 2003). After oxidation, the mixture was diluted with water to about three times of its original volume and subjected to high-speed centrifugal sedimentation to separate the oxidized MWNTs powder (abbreviated as OMWNTs). The powder was washed with distilled water until no residual acid was present and then dried in a vacuum oven at 80 °C for 4 h.

To functionalize the OMWNTs with silane-coupling agents, Shanmugharaj et al. (2007) added APS into the OMWNTs aqueous solution and stirred for 30 min at 80 °C. However, it is well known that in water the organosilane hydrolyzes very quickly to form a trisilanol, which will cause the self-aggregation of trisilanol rather than reacting with the hydroxyl groups on OMWNTs. Hence, we carried out such coupling process in the ethanol solution, which resulted in complete modification and higher yield. In detail, 10 mg OMWNTs were dispersed by ultrasonication in 20 mL of ethanol. Then 1.0 mL of 1.0 wt% APS ethanol solution was added and stirred for 12 h at 40 °C for silanization. The amount of APS used was 1:1 in weight with respect to the OMWNTs. Thereafter, the resultant amino terminated MWNTs were washed with water three times by resuspension/centrifugation to ensure removal of excessive APS. Scheme 1A schematically illustrates the procedure for the silanization of MWNTs.

2.4. Preparation of GOx/AMWNTs multilayer films on the Au electrode

The Au electrode (electrode area 0.032 cm^2) was first abraded with finer grades of SiC paper and polished to a mirror-like surface with 1.0-, 0.3- and 0.05-μm α-Al_2O_3 powder on microcloth pads, followed by rinsing with water and ethanol and briefly cleaning in an ultrasonic bath. The layer forming process started with the introduction of amine functionalities on the Au surface by dipping a clean Au electrode into an aqueous solution of cystamine (10 mg mL^{-1}) in darkness for 2 h. After thiol adsorption, LBL assembly of GOx/AMWNTs was conducted by alternatively dipping the modified electrode into the IO_4^--oxidized GOx solution and the above AMWNTs solution each for 1 h. After each dipping step, the electrode was carefully washed with distilled water for three times to remove the excess of assembling materials and then dried with nitrogen. This sequence was repeated until the desired GOx/AMWNTs bilayer number was obtained. The modified electrode was denoted as Au/CA/$(GOx/AMWNTs)_n$. The assembly process was shown in Scheme 1B. As a control, the multilayer film using OMWNTs was also fabricated under identical conditions. The resulting electrode was abbreviated to Au/CA/$(GOx/OMWNTs)_n$.

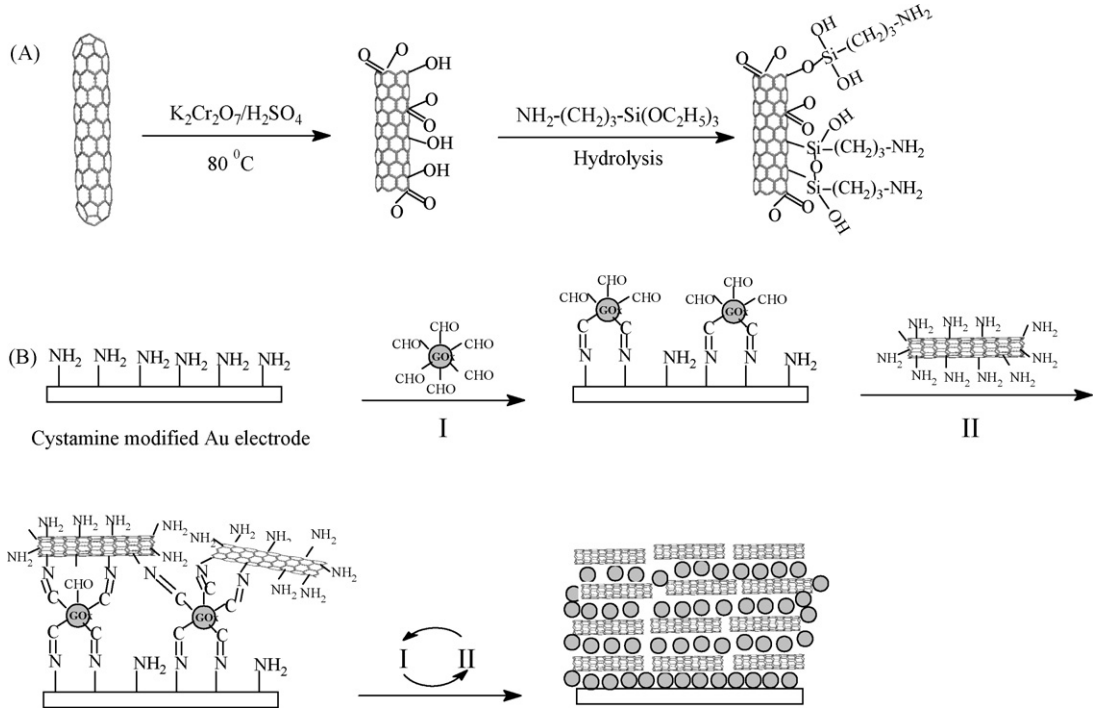

Scheme 1. (A) Processes of interaction between aminosilane and OMWNTs. (B) Stepwise assembly of the Au/CA/(GOx/AMWNTs)$_n$.

For SEM characterization, a silicon wafer was first cleaned in a fresh piranha solution (v/v = 3:7, 30% H_2O_2/98% H_2SO_4) and then thoroughly rinsed with distilled water. The pretreated silicon wafer was placed in a 1% anhydrous toluene solution of APS for 7 min to introduce amino groups. The GOx/AMWNTs multilayer films were then constructed on the silicon wafer by the same procedures as those on the Au electrodes.

3. Results and discussion

3.1. LBL covalent assembly of GOx/AMWNTs multilayer films

Different from other groups' samples in which the nanotubes and enzymes were commonly cast or pasted on the electrode surfaces (Zhang and Gorski, 2005; Chen and Dong, 2007), here we used LBL covalent self-assembly technique to fabricate GOx/AMWNTs multilayer films. The buildup of such supramolecular architecture was constructed as outlined in Scheme 1B. Initially, a base layer of cystamine was chemisorbed on the Au electrode surface via thiol end groups and exposed an array of amino groups towards the solution. Then IO_4^--oxidized GOx molecules were covalently attached to cystamine modified electrode through the formation of Schiff base. Likewise, AMWNTs were linked to IO_4^--oxidized GOx in the same way. The key to this process is the formation of Schiff base between aldehyde groups of IO_4^--oxidized GOx and amino groups of cystamine and AMWNTs. The sequential repetition of the deposition of IO_4^--oxidized GOx and AMWNTs produced homogeneously and stably nanometer-scaled multilayer films with the desired number of GOx/AMWNTs bilayers.

3.2. Characterization of GOx/AMWNTs multilayer films

The assembly and morphology of the GOx/AMWNTs multilayers on a silicon wafer were characterized by SEM. As shown in Fig. 1, randomly oriented AMWNTs covered the entire surface of the silicon wafer. The density of AMWNTs in the first layer was rather small (Fig. 1a) and the nanotubes coverage clearly increased with increasing the number of film assembling (Fig. 1b and c), suggesting the sequential deposition of the AMWNTs onto the substrate. Thus, one may expect to obtain a homogeneous, porous, and three-dimensional GOx/AMWNTs multilayer film with a large surface area provided the assembly procedure was repeated many times. In addition, a close inspection of the AMWNTs grown on the substrate revealed that the AMWNTs, 0.5–1.0 μm in length and 20–80 nm in diameter were most well distributed on the surface, and that most of the anchored AMWNTs were in a form of small bundles or

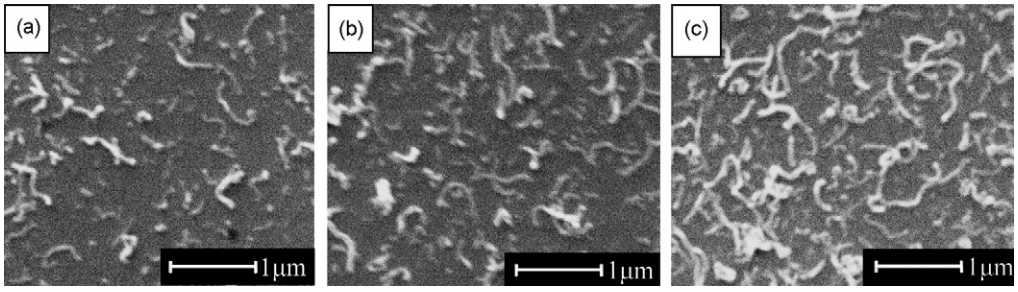

Fig. 1. Representative SEM images of (a) (GOx/AMWNTs)$_1$, (b) (GOx/AMWNTs)$_2$, and (c) (GOx/AMWNTs)$_4$ assembled on a silicon wafer.

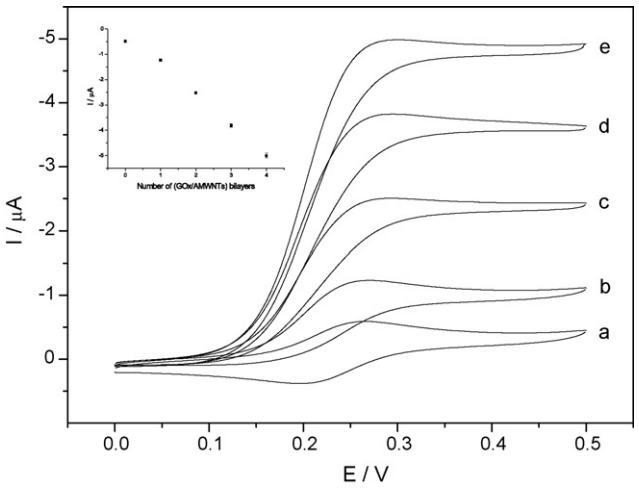

Fig. 2. Cyclic voltammograms of the GOx/AMWNTs multilayer electrodes in the presence of 0.25 mM ferrocenemethanol and 20 mM glucose: (a) zero, (b) one, (c) two, (d) three and (e) four bilayers. Inset: catalytic current versus the number of GOx/AMWNTs bilayers. Error bars have been deduced from measurements in triplicate. Scan rate: 5 mV s^{-1}.

single tubes. This is different from the results of the modified electrode prepared by other methods such as cast coating, mixing CNTs with carbon paste that CNTs existed in the form of agglomerates or indiscernible nanotubes bundles (Luo et al., 2001). Such small bundles and single tubes are believed to be very attractive for the development of glucose biosensor since most of the well-dispersed nanotubes are electrochemically accessible and consequently can be readily and totally used as electrochemical sensing unit. On the other hand, the larger accessible surface area allows more enzyme immobilization compared with that with big bundles of MWNTs, which yields a higher ratio of signal-to-noise for electrochemical determination of glucose. Due to the small particle size (diameter 4–5 nm), the adsorption of GOx onto the AMWNTs cannot be inferred directly from the SEM images. However, from the results of the following electrochemical measurements, it is clear that GOx molecules were present along with the deposited AMWNTs.

The above LBL covalent attachment process was also confirmed by electrocatalytic oxidation of glucose. In the presence of artificial redox mediator (ferrocenemethanol), GOx involved in the multilayer films can electrocatalyze the oxidation of glucose that is expressed as follows (Bourdillon et al., 1993):

$$Fc \rightleftharpoons Fc^{+} + e \quad (1)$$

$$GOx(FAD) + G \underset{k_{-1}}{\overset{k_1}{\rightleftharpoons}} GOx(FAD\text{-}G) \xrightarrow{k_2} GOx(FADH_2) + GL \quad (2)$$

$$GOx(FADH_2) + 2Fc^{+} \xrightarrow{k_3} GOx(FAD) + 2Fc \quad (3)$$

where GOx ($FADH_2$) and GOx (FAD) represent reduced and oxidized forms of GOx, Fc and Fc^{+} are the reduced and oxidized forms of ferrocenyl mediator, and G and GL are β-D-glucose and glucose-D-lactone, respectively. Reaction (1) takes place at the Au electrode surface, charge transport between suitable ferrocene sites through AMWNTs that are in contact with the underlying electrode. The ping-pong enzyme kinetics of GOx are described by reactions (2) and (3). As the potential increases the Fc is oxidized to Fc^{+}, and we observe a catalytic current for the oxidation of glucose. Fig. 2 shows the cyclic voltammetric responses obtained from the Au electrodes modified with different numbers of GOx/AMWNTs bilayers in the presence of 20 mM glucose and 0.25 mM ferrocenemethanol. At a bare Au electrode, a pair of well-reversible redox wave with peak potential separation of 0.06 V was observed (Fig. 2a), which was characteristic of one-electron reversible redox reaction of Fc^{+}/Fc. When a significant amount of active enzyme was covalently attached to the electrodes, well-defined sigmoidal catalytic waves were observed, with an obvious increase in anodic current and an almost complete disappearance of the cathodic current (Fig. 2b–e). As the number of bilayers increased, the electrocatalytic current also enhanced, and that the anodic current showed an almost linear relationship with the number of deposited GOx/AMWNTs bilayers (Inset of Fig. 2). Thus, it is thought that each bilayer contains the same amount of active enzyme, and the GOx/AMWNTs multilayer films are constructed in a uniform growth process, which is well consistent with the SEM results. For comparison, OMWNTs were used instead of AMWNTs for constructing multilayer films. As expected, the electrocatalytic current of the resulting films did not show any enhancement with the increasing number of bilayers (data not shown). This suggested that the multilayer films containing GOx and carbon nanotubes could only be formed successfully through covalent Schiff-base bonding.

In the absence of mass transport limitations, plateau current from the ferrocenemethanol-mediated CVs I_p, is expected to obey the following equation (Anicet et al., 1998):

$$\frac{1}{I_p} = \frac{1}{2FS\Gamma_{ET}}\left(\frac{1}{k_3[Fc]} + \frac{1}{k_2} + \frac{1}{k_{red}[G]}\right) \quad (4)$$

where F is the Faraday 's constant, S is the electrode area, Γ_{ET} is the surface concentration of enzyme, [Fc] is the mediator concentration, [G] is the glucose concentration in the solution, and $k_{red} = k_1k_2/(k_{-1} + k_2)$. I_p was measured from the background-corrected current value by subtracting the glucose-free current to glucose-contain current at a potential of 0.28 V. On the basis of the equation and the known rate constant values ($k_2 = 700\ s^{-1}$, $k_3 = 1.2 \times 10^7\ M^{-1}\ s^{-1}$, $k_{red} = 1.1 \times 10^4\ M^{-1}\ s^{-1}$) (Ehret et al., 1997; Brillas et al., 1997), the surface concentration of GOx deposited at the enzyme electrode was determined, which was 1.29×10^{-12} mol cm^{-2} for the Au/CA/$(GOx/AMWNTs)_1$ and increased to 2.63, 3.99 and 5.30×10^{-12} mol cm^{-2} for the Au/CA/$(GOx/AMWNTs)_2$, Au/CA/$(GOx/AMWNTs)_3$ and Au/CA/$(GOx/AMWNTs)_4$, respectively. It can be seen that Γ_{ET} was linearly dependent on the number of bilayers, and the increment of the amount of GOx (Γ_E) per GOx/AMWNTs bilayer was 1.34×10^{-12} mol cm^{-2}, which was 2-fold higher than that of the multilayer films containing silica nanoparticles and GOx reported in our previous work (Sun et al., 2006). Such a clear increase in the Γ_E value should not be attributed just to the extra active surface area provided by AMWNTs. Actually, the AMWNTs play a dual significant role in both the enzyme immobilization and the transduction events, namely, as carriers for GOx to provide a suitable microenvironment to retain the GOx activity and as a transducer for amplifying the electrochemical signal of the product of the enzymatic reaction, since carbon nanotubes could promote the electron-transfer at the electrochemical interface and may serve as excellent transducers for biosensors (Wang et al., 2003a; Hrapovic et al., 2004). It has been suggested that GOx becomes partially unfolded when associated with CNTs (Liu et al., 2004). This will reduce the tunneling distance of the optimum electron-transfer pathway from the isoalloxazine group in the GOx to a cystamine residue C 164 at the enzyme surface (Alvarez-Icaza et al., 1995), which allows for improved access to the FAD centers by the Fc redox

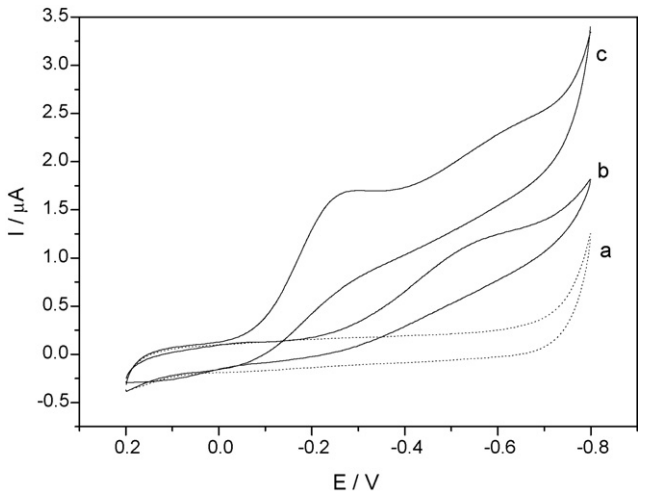

Fig. 3. Typical cyclic voltammograms obtained at Au/CA/(GOx/AMWNTs)$_4$ (a, c) and bare Au electrodes (b) in 0.1 M PBS saturated with N_2 (dotted lines) or air (solid lines). Scan rate: 10 mV s^{-1}.

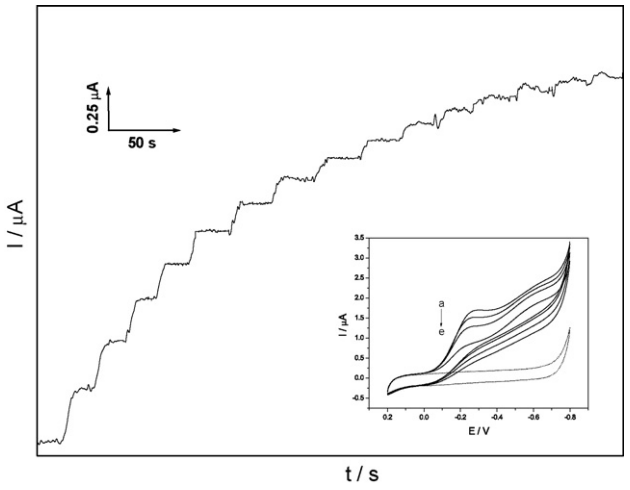

Fig. 4. Amperometric responses of Au/CA/(GOx/AMWNTs)$_4$ electrode at an applied potential of −0.3 V to successive addition of glucose in a stirred 0.1 M PBS in the presence of dissolved oxygen. Inset: cyclic voltammograms of Au/CA/(GOx/AMWNTs)$_4$ in 0.1 M PBS in the absence (e) and presence of dissolved oxygen with (a) 0, (b) 0.5, (c) 1 and (d) 2 mM glucose. Scan rate: 10 mV s^{-1}.

centers. Furthermore, the covalent LBL method we used can provide a tridimensional conductive and porous structure that was confirmed by SEM images. Such porous films would allow the enzyme substrates to enter into the films more easily and have more chance to react with all of the proteins in the films, thus significantly improving the catalytic efficiency compared with the reported values. The facts mentioned above further confirm that the multilayer structure involving AMWNTs and GOx has been formed in a spatially ordered and uniform manner, which offers the possibility of conveniently controlling the active enzyme loading via adjusting the number of the GOx/AMWNTs bilayers attached.

3.3. Electrocatalytic reduction of O_2 at GOx/AMWNTs multilayer electrodes

The need for oxygen reduction at catalytic surfaces has been recognized in fuel cells, batteries, and many other electronic applications (Bard and Faulkner, 1980). Hence, oxygen reduction at nanotube surfaces is of great interest. Fig. 3 depicts cyclic voltammograms for dissolved oxygen reduction at the Au/CA/(GOx/AMWNTs)$_4$ and bare Au electrodes in 0.1 M PBS. When the Au/CA/(GOx/AMWNTs)$_4$ was in N_2-saturated solution, no redox peak in the potential range 0.2 to −0.8 V were observed (curve a). While in the presence of O_2, a remarkable catalytic reduction peak appeared at −0.28 V (curve c), which was documented to be a two-electron reduction process to produce hydrogen peroxide (Eq. (5)) (Bockris and Srinivasan, 1969; Bard and Faulkner, 1980). As a control, the reduction of oxygen on the bare Au electrode resulted in an ill-defined peak at about −0.55 V with smaller current, shown in Fig. 3b. Compared with the bare electrode, the Au/CA/(GOx/AMWNTs)$_4$ not only improves the reduction currents of O_2 but also decreases the overvoltage by at least 0.28 V, which indicates a more facile reaction occurring at the multilayer films. This result is consistent with literature for other CNTs modified electrode (Britto et al., 1999; Dai and Shiu, 2004), demonstrating that the present strategy of using the covalent functionalization does not affect the inherent electrochemical properties of CNTs, and CNTs retain excellent electrocatalytic ability towards reduction of O_2. The larger lowering of the overvoltage observed in the presence of CNTs is attributed to the oxide defects on the tube sidewalls and ends which can be involved in the redox reaction and makes CNTs more hydrophilic so that the sample can contact the surface better (Zhang et al., 2004).

3.4. Electrocatalytic oxidation of glucose at Au/CA/(GOx/AMWNTs)$_n$

The electrocatalytic oxidation of glucose depicted by Eqs. (1)–(3) is carried out with the help of an artificial redox mediator, ferrocenemethanol. This mediator does enhance electron-transfer efficiency between immobilized GOx and the electrode. However, due to the mediator presented in solution, the modified electrodes would be contaminative and irreproducible for continuous use (Coche-Guerente et al., 1997). Since AMWNTs assembled on the modified electrodes could enhance the reduction activity of dissolved oxygen, decreasing the reductive overvoltage along with the increased current signal, the dissolved oxygen can be used as the electron-transfer mediator (Zhang et al., 2007). In the presence of dissolved oxygen the oxidation of glucose follows Eq. (6):

$$O_2 + 2H^+ + 2e^- \rightarrow H_2O_2 \quad (5)$$

$$G + O_2 + 2H + \xrightarrow{GOx} GL + H_2O_2 \quad (6)$$

where G and GL are β-D-glucose and glucose-D-lactone, respectively. The consumption of dissolved oxygen led to the decrease of O_2 concentration. Therefore, a glucose biosensor can be developed based on the detection of O_2 reductive signal changes resulting from the addition of glucose. Inset of Fig. 4 shows cyclic voltammograms of the Au/CA/(GOx/AMWNTs)$_4$ in air-saturated PBS with (a) 0 mM, (b) 0.5 mM (c) 1.0 mM and (d) 2.0 mM glucose. We can see that the reduction peak current of O_2 decreased with the addition of glucose, suggesting the feasibility of our strategy.

Amperometric response curves of Au/CA/(GOx/AMWNTs)$_4$ for the successive additions of 1.0 mM glucose in air-saturated PBS are presented in Fig. 4. Considering the best signal-to-noise ratio, the measurements were performed at an applied potential of −0.3 V. The reaction occurring at the biosensor was very fast in reaching a dynamic equilibrium upon each addition of the glucose solution, generating a steady-state current signal within 10 s. Such shorter response time was indicative of faster charge transport in films with AMWNTs. The current reached a saturation value at high glucose concentration, showing the characteristics of the Michaelis–Menten kinetics. Based on the amperometric response, a calibration curve was obtained in Fig. 5(c). The linear calibration range was extended up to 7.0 mM with a correlation coefficient of

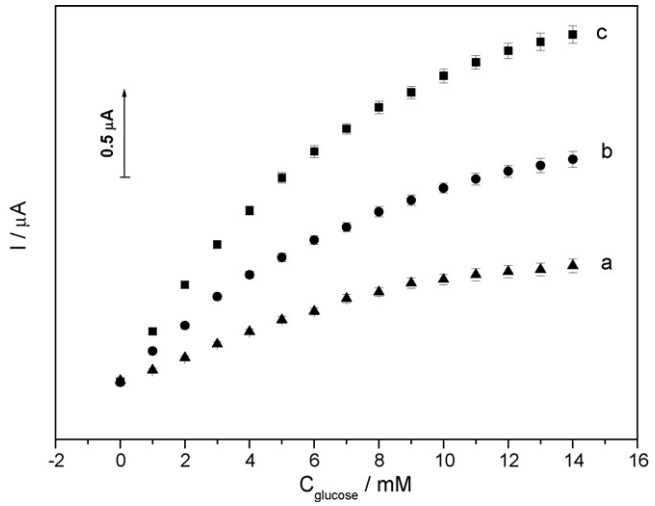

Fig. 5. Calibrations for the number of GOx/AMWNTs bilayers as a function of glucose concentration: (a) Au/CA/(GOx/AMWNTs)$_2$, (b) Au/CA/(GOx/AMWNTs)$_3$ and (c) Au/CA/(GOx/AMWNTs)$_4$. Bioelectrocatalytic signal values were obtained from respective current-time curves. Error bars have been deduced from measurements in triplicate.

0.996. Such extended linear range might arise from two effects: oxygen reduction promoted by AMWNTs and the porous multilayer film through which the substrates can penetrate. The sensitivity obtained was of 7.46 μA mM^{-1} cm^{-2}, which is higher than that 3.9 μA mM^{-1} cm^{-2} at Au nanoparticles-GOx multilayer biosensor and 5.6 μA mM^{-1} cm^{-2} reported for GOx/SDS-MWNTs biosensors fabricated using the PDDA cross-linker (Zhao et al., 2005; Yan et al., 2007). A detection limit of 8.0 μM can be estimated based on the signal-to-noise characteristics of these data (S/N = 3). The high sensitivity is accompanied by a low noise level, allowing convenient detection of micromolor concentrations.

The amperometric response and the sensitivity of the fabricated biosensors to glucose are related to the bilayer numbers of GOx/AMWNTs. Fig. 5 shows the calibration curves obtained from the electrodes modified with different numbers of GOx/AMWNTs bilayers. The sensitivity calculated from the linear region of calibration curve was 2.27 μA/mM cm^2 for the Au/CA/(GOx/AMWNTs)$_2$ and increased to 4.95 and 7.46 μA/mM cm^2 for the Au/CA/(GOx/AMWNTs)$_3$ and Au/CA/(GOx/AMWNTs)$_4$, respectively. Even higher sensitivity may be achieved by increasing the numbers of attached bilayers. Hence, the analytical performance of the Au/CA/(GOx/AMWNTs)$_n$ can be adjusted by modulating the deposition number of GOx/AMWNTs bilayers. This is the obvious difference from other methods to prepare CNTs-based glucose biosensor, in which GOx was only immobilized in a monolayer of CNTs, thus the amperometric response could not be controlled (Lin et al., 2004; Lim et al., 2005). The ability to control the analytical performance of the electrode should be useful, especially for the electrode containing multiple enzymes with significantly different activities.

3.5. Interference study and the stability

The general problem in the electrochemical detection of glucose is the interference from redox-active species such as ascorbic acid (AA), uric acid (UA) and acetaminophen, which are usually coexist with glucose in physiological samples. Here, a comparative study was made between the current obtained for the concentration of 0.1 mM AA, 0.1 mM UA and 1 mM acetaminophen, and that obtained for 1.0 mM glucose at the applied potential of −0.3 V. The injection of 1.0 mM glucose caused an immediate decrease of the reduction current, while subsequent injection of those three compounds did not cause any interference on the current response (not shown here). The use of lower detection potential greatly reduced the responses of common interference. Hence, highly selective response to glucose was obtained without any artificial mediator or perm-selective membrane. This is an advantage of the proposed biosensor over those reported previously (Wang and Musameh, 2003b; Lim et al., 2005).

Stability of a modified electrode is an essential issue for the practical applications. The long-term storage stability of the GOx/AMWNTs multilayer electrodes was investigated when stored at 4 °C and measured at intervals over several days. No obvious decrease in the response to glucose was observed after 3 weeks and it retained about 90% of its original sensitivity after 1 month. Moreover, the sensor kept a constant current when successively swept for 100 cycles in the presence of glucose, indicating good operational stability. Such excellent stability is attributed to the strong covalent interaction between AMWNTs and GOx, which is not affected by the changes such as the ionic strength, the solution pH, and temperature. Furthermore, the carboxylic acids on AMWNTs, which were introduced by acid treatment, could also stabilize the adsorbed GOx through the formation of hydrogen bonds, since there are plenty of hydroxyl and carboxylic groups (carbohydrate) on the surface of GOx (Wang et al., 2003c).

4. Conclusion

This work is the first attempt to apply the amino terminated MWNTs to glucose biosensors via layer-by-layer covalent self-assembly method without any cross-linker between the AMWNTs and GOx. Based on the silane treatment, APS molecules containing amino-ended groups were covalently bonded on OMWNTs through Si–O–C linkages. Such amino-termination of AMWNTs can be reacted with the aldehyde groups of IO_4^--oxidized GOx through the formation of Schiff base. The resulting multilayer film showed a porous structure and the assembled AMWNTs exhibited an electrocatalytic activity to the reduction of dissolved oxygen, which facilitated convenient low-potential stable detection of the glucose. AMWNTs involved play multiple roles: (1) to act as substrate for GOx immobilization, (2) to electrocatalytically reduce O_2 at the AMWNTs surface, and (3) to enhance measurement signal because of its fast electron-transfer and large working surface area. Above all, the catalytic response of the resulting GOx/AMWNTs electrodes to glucose enhanced significantly with increasing number of the bilayers, indicating that the sensitivity is tunable by controlling the film thickness. Due to the relative low applied potential, the interference from other electro-oxidizable compounds (such as uric acid and ascorbic acid) was minimized obviously, which improved the selectivity of the biosensors. Furthermore, the mild fabrication process, covalent attachment technology and active role of the presence of the AMWNTs overcome the drawback on stability of multilayer films based on layer-by-layer electrostatic adsorption technique. Hence, such GOx/AMWNTs electrodes could be used as accurate, rapid, and inexpensive glucose concentration.

Acknowledgement

This work was supported by Key Laboratory for Supramolecular Structure and Materials of Ministry of Education, Jilin University.

References

Anicet, N., Bourdillon, N.C., Moiroux, J., Saveant, J.M., 1998. The Journal of Physical Chemistry B 102, 9844–9849.

Alvarez-lcaza, M., Kalisz, H.M., Hecht, H.J., Aumann, K.D., Schomburg, D., Schmid, R.D., 1995. Biosensors & Bioelectronics 10, 735–742.
Bard, A.J., Faulkner, L.R., 1980. Electrochemical Methods. Wiley, New York.
Baughman, R.H., Zakhidov, A.A., de Heer, W.A., 2002. Science 297, 787–792.
Bockris, J.O.M., Srinivasan, S., 1969. Fuel Cells: Their Electrochemistry. Mcgraw-Hill, New York.
Bourdillon, C., Demaille, C., Gueris, J., Moiroux, J., Savéant, J., 1993. Journal of the American Chemical Society 115, 12264–12269.
Brillas, E., Cabot, P.L., Garrido, A., Montilla, M., Rodriguez, R.M., Carrasco, J., 1997. Journal of Electroanalytical Chemistry 430, 133–140.
Britto, P.J., Santhanam, K.S.V., Rubio, A., Alonso, J.A., Ajayan, P.M., 1999. Advanced Materials 11, 154–157.
Chen, H.J., Dong, S.J., 2007. Biosensors & Bioelectronics 22, 1811–1815.
Coche-Guerente, L., Cosnier, S., Labbe, P., 1997. Chemistry of Materials 9, 1348–1352.
Dai, Y.Q., Shiu, K.K., 2004. Electroanalysis 16, 1697–1703.
Decher, G., 1997. Science 277, 1232–1237.
Deng, L., Liu, Y., Yang, G., Shang, L., Wen, D., Wang, F., Xu, Z., Dong, S., 2007. Biomacromolecules 8, 2063–2071.
Ehret, R., Baumann, W., Brischwein, M., Schwinde, A., Stegbauer, K., Wolf, B., 1997. Biosensors & Bioelectronics 12, 29–41.
Fan, S., Chapline, M.G., Franklin, N.R., Tombler, T.W., Cassell, A.M., Dai, H., 1999. Science 283, 512–514.
Fuhrer, M.S., Nygard, J., Shih, L., Forero, M., Yoon, Y.G., Mazzoni, M.S.C., Choi, H.J., Ihm, J., Louie, S.G., Zettl, A., Mceuen, P.L., 2000. Science 288, 494–497.
Guan, W.J., Li, Y., Chen, Y.Q., Zhang, X.B., Hu, G.Q., 2005. Biosensors & Bioelectronics 21, 508–512.
Hrapovic, S., Liu, Y., Male, K.B., Luong, J.H.T., 2004. Analytical Chemistry 76, 1083–1088.
Huang, X.J., Im, H.S., Yarimaga, O., Kim, J.H., Lee, D.H., Kim, H.S., Chio, Y.K., 2006. The Journal of Physical Chemistry B 110, 21850–21856.
Iijima, S., 1991. Nature 354, 56–58.
Jiang, C.Y., Tsukruk, V.V., 2006. Advanced Materials 18, 829–840.
Joshi, P.P., Merchant, S.A., Wang, Y., Schmidtke, D.W., 2005. Analytical Chemistry 77, 3183–3188.
Lim, S.H., Wei, J., Lin, J., Li, Q., Kua, Y.J., 2005. Biosensors & Bioelectronics 20, 2341–2346.
Lin, Y., Lu, F., Tu, Y., Ren, Z., 2004. Nano Letters 4, 191–195.
Liu, J.Q., Paddon-Row, M.N., Gooding, J.J., 2004. The Journal of Physical Chemistry B 108, 8460–8466.
Luo, H.X., Shi, Z.J., Li, N.Q., Gu, Z.N., Zhuang, Q.K., 2001. Analytical Chemistry 73, 915–920.
Olek, M., Ostrander, J., Jurga, S., Mohwald, H., Kotov, N., Kempa, K., Giersig, M., 2004. Nano Letters 4, 1889–1895.
Rao, C.N.R., Satishkumar, B.C., Govindaraj, A., Nath, M., 2001. Chemphyschem 2, 78–105.
Ravindran, S., Chaudhary, S., Colburn, B., Ozkan, M., Ozkan, C.S., 2003. Nano Letters 3, 447–453.
Salimi, A., Compton, R.G., Hallaj, R., 2004. Analytical Biochemistry 333, 49–56.
Shanmugharaj, A.M., Bae, J.H., Lee, K.Y., Noh, W.H., Lee, S.H., Ryu, S.H., 2007. Composites Science and Technology 67, 1813–1822.
Sun, Y.Y., Yan, F., Yang, W.S., Sun, C.Q., 2006. Biomaterials 27, 4042–4049.
Sun, Y.Y., Yan, F., Yang, W.W., Yang, W.S., Sun, C.Q., 2007. Analytical and Bioanalytical Chemistry 387, 1565–1572.
Wang, J., Kawde, A., Mustafa, M., 2003a. Analyst 128, 912–916.
Wang, J., Musameh, M., 2003a. Analytical Chemistry 75, 2075–2079.
Wang, J., Musameh, M., 2003b. Analyst 128, 1382–1385.
Wang, J., Musameh, M., 2005. Analytica Chimica Acta 539, 209–213.
Wang, J., Musameh, M., Lin, Y., 2003b. Journal of the American Chemical Society 125, 2408–2409.
Wang, S.G., Zhang, Q., Wang, R., Yoon, S.F., 2003c. Biochemical and Biophysical Research Communications 311, 572–576.
Wong, S.S., Joselevich, E., Woolley, A.T., Cheung, C.L., Lieber, C.M., 1998. Nature 394, 52–57.
Yan, X.B., Chen, X.J., Tay, B.K., Khor, K.A., 2007. Electrochemistry Communications 9, 1269–1275.
Zaborsky, O.R., Ogletree, J., 1974. Biochemical and Biophysical Research Communications 61, 210–216.
Zhang, J.D., Feng, M.L., Tachikawa, H., 2007. Biosensors & Bioelectronics 22, 3036–3041.
Zhang, M., Yan, Y., Gong, K., Mao, L., Guo, Z., Chen, Y., 2004. Langmuir 20, 8781–8785.
Zhang, M.G., Gorski, W., 2005. Analytical Chemistry 77, 3960–3965.
Zhao, H., Ju, H., 2006. Analytical Biochemistry 350, 138–144.
Zhao, W., Xu, J.J., Chen, H.Y., 2005. Frontiers of Bioscience 10, 1060–1069.